

# Criticality of lateral inhibition for edge enhancement in neural systems

Pradeep Arkachar, Meghanad D. Wagh\*

*Department of Electrical and Computer Engineering, Lehigh University, Bethlehem, PA 18015, USA*

Received 19 December 2004; received in revised form 8 March 2006; accepted 20 March 2006

Communicated by V. Jirsa

Available online 13 October 2006

## Abstract

Although the role of lateral inhibition in edge (contrast) enhancement is well known, it has not been parametrized. This paper investigates the imbalance between the lateral inhibitory and excitatory stimuli and its effect on the edge enhancement and stability. It is shown that this imbalance can be expressed through  $\gamma$ , a ratio of inhibitory to excitatory weights in a neuron. Stability requires  $\gamma$  to be less than the *critical ratio*  $\Theta$ . As  $\gamma$  approaches  $\Theta$ , edge enhancement increases, the rise being the sharpest just before instability. The increase in edge enhancement is also accompanied by an increase in the lateral spread of perturbations across the neuron layer.

© 2006 Elsevier B.V. All rights reserved.

*Keywords:* Neural system; Lateral inhibition; Edge enhancement; Stability; Contrast enhancement

## 1. Introduction

Lateral inhibition refers to the phenomenon where a neuron in a neural network inhibits its neighbors, thus creating a competition between neurons. This phenomenon is observed in the visual cortex [9,5] as well as auditory cortex [7,19]. The role of inhibition in contrast enhancement has been recognized for a long time. Ernst Mach, a 19th century physicist, observed that retinal inhibition accentuates contours and borders in the visual field. This finding received a boost by the experimental work of Hartline and Ratliff on the eyes of horseshoe crab *Limulus* [9]. They observed that when illuminated, the retinal cells are excited by the light within a central area and inhibited by light in the surrounding area. This resulted in the enhancement of the edges or contours between the regions of different intensities. This effect is called edge or contrast enhancement.

A number of researchers have studied lateral inhibition and its role in edge enhancement and stability of neural networks. In 1990, Kelly showed that large imbalance between the excitatory and inhibitory stimulus can cause

instability in neural networks [12]. Later, Shadlen and Newsome [17,16] proved that relative strengths of excitatory and inhibitory inputs are important to stabilize neural response. Their research indicates that neurons avoid saturation by balancing excitation with inhibition. Their analysis of high-input regime, where integrate-and-fire neurons receive a large number of both excitatory and inhibitory inputs, showed that such a balance is responsible for the dynamic range of neurons' response. Burkitt [3] has also shown that balanced inhibition with reversal potential can resolve the problem of dynamic range of neural response. Amit and Brunel [1] have shown that cortical network of integrate-and-fire neurons with balanced inhibition and excitation and stochastic background is stable. Simulations of Gutkin and Smith [8] have further strengthened the argument that the right amount of lateral inhibition is critical to the stability of cortical neural networks as well as to edge enhancement. Their work shows that a recurrent cortical neural network reaches a steady state and enhances the edges only in the presence of weak lateral inhibition.

Thus, the balance between the inhibitory and the excitatory characteristics of a neuron and its impact on the stability and edge enhancement is well documented. But no results pertaining to quantitative estimates of the imbalance that cause the instability are available. In this

\*Corresponding author. Tel.: +1 610 7584142; fax: +1 610 7586279.

E-mail addresses: [pradeep@Alumni.Lehigh.Edu](mailto:pradeep@Alumni.Lehigh.Edu) (P. Arkachar), [mdw0@Lehigh.Edu](mailto:mdw0@Lehigh.Edu) (M.D. Wagh).

paper, we consider a planar neural network with lateral inhibition. We show that the stability and the edge enhancement of this network is governed by  $\gamma$ , the ratio of the inhibitory to excitatory strengths. In particular, when  $\gamma$  is less than the *critical ratio*  $\Theta$ , the network is stable. The bound  $\Theta$  is only dependent upon the model and the connectivity of the network. Further, when the network is stable, its edge enhancement increases with  $\gamma$  and becomes very large when  $\gamma$  nears  $\Theta$ .

## 2. Model of the neural system

Neural network analysis and simulation is generally difficult because the number of neurons that influence each other is very large. Previous research has shown the columnar organization of neurons, i.e., groups of similar neurons behave like single neurons (see review article [15]). We take advantage of this fact to partition the retinal neurons within a layer into large clusters of neighboring neurons. Each of these clusters represents a single neuron in our model. Thus, the response of each of our neurons is an aggregate of the responses of all the neurons in the corresponding cluster. This model influences our analysis in two ways. Firstly, even though individual neurons may be integrate-and-fire type with spikes at the output, the composite output of a large number of such neurons can be considered continuous. Further, it also allows us to ignore threshold while computing the neuron output since that output is the result of the collective behavior of a large number of neurons. Thus the neurons in our model exhibit linear behavior.

There is substantial amount of evidence that dendrites develop randomly and consequently real neural networks have a random structure which is extremely difficult to analyze except in a stochastic manner [3,4]. In our model, we hypothesize that the probability of neuron connectivity depends upon the proximity. In other words, the number of connections across the clusters of neurons (which represent our aggregate neurons) is a function of the physical distance between the clusters. We realize the interconnection density between the clusters through the weight of the connections between our neurons. Thus, both the excitatory and the inhibitory weights of our neuron connections can be assumed to be functions of the distance between the clusters that the neurons represent.

Our model differs from models used by earlier researchers substantially. In particular, our representation of neuron clusters as single neurons allows us to use simpler (linear) model of an individual neuron, while allowing for a more detailed network topology. In much of the previous research in this area, the network topology was not a consideration. Burkitt, for example, deals with a stochastic distribution of neurons [3]. We use a simpler model of the cortical networks consisting of neurons laid out uniformly in space. Each neuron provides lateral inhibition to certain range of its neighbors. We use a linear model of a neuron. Several previous papers [14,6,5] have considered neurons in

primary visual cortex to be linear cells that compute a weighted sum of light intensities falling on the receptive field. Evidence is also available showing that the P cells, a type of retinal ganglion cells, behave linearly for small variations in the stimulus [13,2]. Even though our network geometry closely resembles that of Gutkin and Smith [8] and Kelly [12], they use sigmoid or other non-linear functions to compute the neuron response against our linear function. Further, the connection matrix used in [12] is a cyclic Toeplitz matrix and is quite different from the one we have employed. Finally, unlike others, our weights are functions of the distance between the source and destination nodes with the inhibitory weight of an edge of the same length being a constant  $\gamma$  times the weight of an excitatory edge.

Our model of neuron network shown in Fig. 1 closely resembles the arrangement of retinal neurons. It could be considered a logical representation of the retinal pathway with the excitatory input coming from the rods/cones and inhibitory inputs coming from lateral horizontal cells. The sole purpose of the horizontal cells is to inhibit the neurons they synapse with. This is responsible for a lateral inhibition in the cortical network in the eyes. The output of our neural system is then applied to bipolar cells and finally to ganglion cells.

The assumptions and notation used in this paper are as follows.

- The  $N$  denotes the number of identical neurons in the array as shown in Fig. 1. Each of our neurons in Fig. 1 represents a cluster of real neurons.
- Each neuron has  $n_e$  excitatory input connections from the neurons in the lower layer and  $n_i$  inhibitory input connections from neurons in its own layer (lateral connections). We assume that the weight of a connection is a function of the distance between the source and the destination neurons. A neuron is affected the same way by neurons equidistant from it on either side. The excitatory weights are denoted by  $w_j$  where  $j$  is the difference in the source and the destination neuron indices. The inhibitory weights are assumed to follow

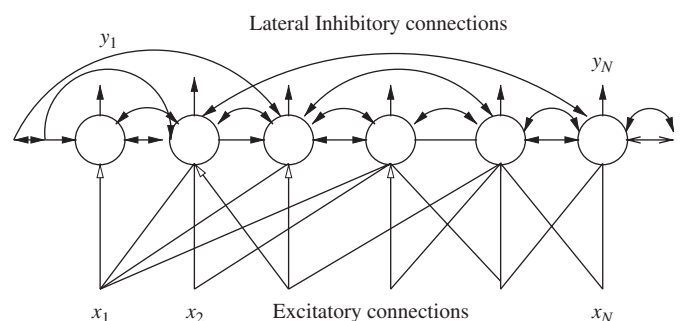


Fig. 1. The logical representation of the neural network in retina. The excitatory inputs ( $x_i$ 's) come from the photoreceptors and lateral inhibitory inputs represent the collections of horizontal cells. The  $y_i$ 's represent the outputs of neurons.

the same function of distance as the excitatory weights. The proportions of the inhibitory and the excitatory neurons in the cluster are responsible for the relative strengths of the inhibitory and excitatory behavior of the entire cluster. To account for this, we scale the inhibitory weights by the *weight ratio*  $\gamma$ . The  $\gamma$  allows one to compare the populations of the inhibitory and the excitatory neurons within a cluster. Thus, the inhibitory weight of an edge between neurons  $j'$  away is denoted by  $\gamma w'_j$  where the part of inhibitory weight that depends upon the distance is  $w'_j$ . Fig. 2 shows the weights of the connections from a single neuron.

- In the analysis we have ignored self-inhibition. In other words,  $w'_0$  was set to 0. But it should be pointed out that the presence of self-inhibition does not change the overall behavior of the system, though it reduces the edge enhancement. All the simulations reported in Section 4 use self-inhibition.
- In order to minimize the edge effects due to a finite array of neurons, we reflect the connections at the end of the array. In other words, if the  $j$ th neighbor of a neuron is outside the range of neurons under consideration, then the weight of the connection from its mirror image (from the array edge) is doubled. As long as the discontinuities in the input stimulus are sufficiently away from the edge, this is sufficient to suppress the edge effects of the finite array.
- The input stimulus at time  $t$  is denoted by  $x_i(t)$ ,  $1 \leq i < N$ .
- In order to produce a constant (and equal) output corresponding to a constant input, we scale the output of each neuron by a *normalization factor*  $\eta$ . It is shown later that  $\eta$  is inversely proportional to the sum of all the excitatory and the inhibitory weights.
- We assume a linear time-invariant neural system. Thus, our weights are constant over time and are independent of either the excitation or the output.

Based on the model described above, the discrete-time output  $y_i$  of the  $i$ th neuron at time  $t + 1$  is given by

$$y_i(t + 1) = \eta \left[ \sum_{j=-\rho}^{\rho} w_{|j|} x_{i+j}(t) - \gamma \sum_{j=-\tau}^{\tau} w'_{|j|} y_{i+j}(t) \right], \quad (1)$$

where  $\rho = (n_e - 1)/2$  and  $\tau = (n_i - 1)/2$ . It should be noted here that because of the infinite array assumption stated

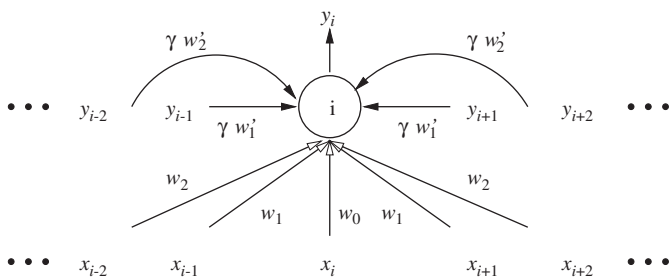


Fig. 2. Connections to the  $i$ th neuron. The lateral inhibitory weight of the edges coming from neurons  $i + t$  and  $i - t$  is  $\gamma w'_t$ . Weight of the edges from inputs  $x_{i+t}$  and  $x_{i-t}$  is  $w_t$ . There is no self-inhibition, i.e.,  $w'_0 = 0$ .

above, if the index  $i + j$  of  $x$  or  $y$  in (1) goes out of its defined range of  $1 - N$ , then it needs to be reflected with respect to the neuron index, i.e., an out of range index  $j$  needs to be changed to  $2i - j$ . For example, when  $n_e = n_i = 5$ , the output of the second neuron,  $y_2$  is

$$y_2(t + 1) = \eta [w_2 x_4(t) + w_1 x_1(t) + w_0 x_2(t) + w_1 x_3(t) + w_2 x_4(t) - \gamma (w'_2 y_4(t) + w'_1 y_1(t) + w'_1 y_3(t) + w'_2 y_4(t))].$$

Eq. (1) can also be written in the following matrix form:

$$\mathbf{Y}(t) = \eta [\mathbf{A}\mathbf{X}(t) - \gamma \mathbf{B}\mathbf{Y}(t - 1)], \quad (2)$$

where  $\mathbf{X} = (x_1, x_2, \dots, x_N)^T$ ,  $\mathbf{Y} = (y_1, y_2, \dots, y_N)^T$  and  $\mathbf{A}$  and  $\mathbf{B}$  are  $N \times N$  square matrices:

$$\mathbf{A} = \begin{pmatrix} w_0 & 2w_1 & 2w_2 & \dots & 2w_\rho & 0 & \dots \\ w_1 & w_0 & w_1 & 2w_2 & \dots & 0 & 0 \\ \vdots & \vdots & \vdots & \vdots & \vdots & \vdots & \vdots \\ 0 & w_\rho & \dots & w_0 & \dots & w_\rho & \dots \\ \vdots & \vdots & \vdots & \vdots & \vdots & \vdots & \vdots \\ 0 & \dots & \dots & 2w_2 & w_1 & w_0 & w_1 \\ \dots & 0 & 0 & \dots & \dots & 2w_1 & w_0 \end{pmatrix},$$

$$\mathbf{B} = \begin{pmatrix} 0 & 2w'_1 & \dots & 2w'_\tau & \dots & 0 & 0 \\ w'_1 & 0 & w'_1 & 2w'_2 & \dots & 0 & 0 \\ \vdots & \vdots & \vdots & \vdots & \vdots & \vdots & \vdots \\ \dots & w'_\tau & \dots & 0 & \dots & w'_\tau & \dots \\ \vdots & \vdots & \vdots & \vdots & \vdots & \vdots & \vdots \\ 0 & \dots & \dots & \dots & w'_1 & 0 & w'_1 \\ 0 & 0 & 2w'_\tau & \dots & \dots & 2w'_1 & 0 \end{pmatrix}.$$

Fig. 3 represents a linear feedback system based on Eq. (2). Because of our assumption that the weights and connectivity are constant, this is a time-invariant system. It will be shown in the subsequent sections that  $\gamma$  should be less than  $\Theta$  for a stable output.

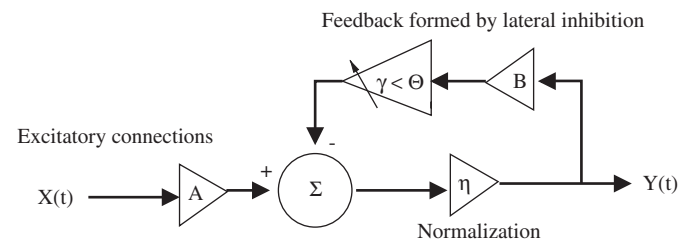


Fig. 3. The neural network of Fig. 1 represented as a linear time-invariant feedback system from Eq. (2).

### 3. Mathematical analysis of the neural system

#### 3.1. Normalization

We use a constant *normalization factor*,  $\eta$ , in our analysis such that if the input stimulus,  $x_i$ , is constant over time at some value, then the output also settles at that same value. Let  $x_i = x$  for all  $i$ . Then, the output  $y$  of each neuron is obtained from (1) as

$$y = \eta \left[ \sum_{j=-\rho}^{\rho} w_{|j|} x - \gamma \sum_{k=-\tau}^{\tau} w'_{|k|} y \right]. \tag{3}$$

From (3) we get  $\eta$  as

$$\eta = \frac{1}{\sum_{j=-\rho}^{\rho} w_{|j|} - \gamma \sum_{k=-\tau}^{\tau} w'_{|k|}} \tag{4}$$

$$= \frac{1}{\text{Sum of excitatory weights} - \text{sum of lateral inhibitory weights}}. \tag{5}$$

#### 3.2. Critical ratio

Let  $\lambda_i, i = 1, \dots, N$ , denote the eigenvalues of  $\mathbf{B}$ . The characteristic equation of  $\mathbf{B}$  is given by

$$|\mathbf{B} - \lambda \mathbf{I}| = 0.$$

Let us denote the sum of each row in  $\mathbf{B}$  as  $S$ . In the above determinant, after adding the first  $N - 1$  columns to the last column, we get the equivalent equation

$$\begin{vmatrix} -\lambda & 2w'_1 & \dots & 2w'_\tau & \dots & 0 & S - \lambda \\ w'_1 & -\lambda & w'_1 & 2w'_2 & \dots & 0 & S - \lambda \\ \vdots & \vdots & \vdots & \vdots & \vdots & \vdots & \vdots \\ \dots & w'_\tau & \dots & -\lambda & \dots & w'_\tau & \dots \\ \vdots & \vdots & \vdots & \vdots & \vdots & \vdots & \vdots \\ 0 & \dots & \dots & \dots & w'_1 & -\lambda & S - \lambda \\ 0 & 0 & 2w'_\tau & \dots & \dots & 2w'_1 & S - \lambda \end{vmatrix} = 0.$$

One can see that by setting  $\lambda = S$ , the last column of the determinant becomes 0 indicating that one of the eigenvalues is

$$\lambda_m = S. \tag{6}$$

From Gerschgorin's circle theorem [18], all the eigenvalues lie within or on the boundary of the circles whose radii are the sum of absolute values of all entries in each row except the value on the principal diagonal. Applying this to matrix  $\mathbf{B}$ , we get

$$|\lambda_i| \leq S, \quad i = 1, 2, \dots, N. \tag{7}$$

From (6) and (7),  $\lambda_m$  is the maximum eigenvalue of  $\mathbf{B}$ . Consider now the system equation given by (2). Assume that the system outputs are zero before the stimulus is applied. This system is causal because as shown in (2), the output of the system at time  $t$  is only dependent upon its

inputs and outputs till time  $t$ . Let the stimulus  $\mathbf{X}$  be constant over time. Then we have

$$\mathbf{Y}(0) = 0,$$

$$\mathbf{Y}(1) = \eta \mathbf{A} \mathbf{X}.$$

By using recursion for solving Eq. (2) we get

$$\begin{aligned} \mathbf{Y}(t) &= \eta [\mathbf{A} \mathbf{X} - \gamma \mathbf{B} \mathbf{Y}(t-1)] \\ &= \eta [\mathbf{I} - \gamma \eta \mathbf{B} + \dots + (-1)^{t-1} (\gamma \eta \mathbf{B})^{t-1}] \mathbf{A} \mathbf{X} \\ &= \eta \mathbf{C} \mathbf{A} \mathbf{X}, \end{aligned} \tag{8}$$

where

$$\begin{aligned} \mathbf{C} &= [\mathbf{I} - \gamma \eta \mathbf{B} + \dots + (-1)^{t-1} (\gamma \eta \mathbf{B})^{t-1}] \\ &= [\mathbf{I} + (-1)^{t-1} (\gamma \eta \mathbf{B})^t] [\mathbf{I} + \gamma \eta \mathbf{B}]^{-1}, \end{aligned} \tag{9}$$

provided none of the eigenvalues  $\lambda$  satisfy  $\gamma \eta \lambda = -1$ . Eq. (9) can be verified by noting that

$$\mathbf{C} [\mathbf{I} + \gamma \eta \mathbf{B}] = [\mathbf{I} + (-1)^{t-1} (\gamma \eta \mathbf{B})^t],$$

and that the matrix  $[\mathbf{I} + \gamma \eta \mathbf{B}]$  is invertible if no eigenvalue  $\lambda$  of  $\mathbf{B}$  equals  $-(\gamma \eta)^{-1}$ . Combining (8) and (9) one gets

$$\mathbf{Y}(t) = \eta [\mathbf{I} + (-1)^{t-1} (\gamma \eta \mathbf{B})^t] [\mathbf{I} + \gamma \eta \mathbf{B}]^{-1} \mathbf{A} \mathbf{X}.$$

As  $t \rightarrow \infty$ , the geometric progression,  $\mathbf{C}$ , converges if and only if  $|\gamma \eta \lambda_m| < 1$ . Therefore, the steady-state output is

$$\mathbf{Y}(\infty) = \eta [\mathbf{I} + \gamma \eta \mathbf{B}]^{-1} \mathbf{A} \mathbf{X}.$$

The neural system would be stable only if the output  $\mathbf{Y}$  converges asymptotically. By substituting values of  $\eta$  and  $\lambda_m$  from (4) and (6) in the inequality, we deduce that for stability, one should have

$$\left| \frac{\gamma \sum_{j=-\tau}^{\tau} w'_{|j|}}{\sum_{j=-\rho}^{\rho} w_{|j|} - \gamma \sum_{j=-\tau}^{\tau} w'_{|j|}} \right| < 1. \tag{10}$$

We assume that the lateral inhibition effect is less than the overall excitatory effect, so as to produce a meaningful output. Since the ratio in (10) is positive, we get the condition for a stable output to be

$$\gamma < \frac{\sum_{j=-\rho}^{\rho} w_{|j|}}{2 \sum_{j=-\tau}^{\tau} w'_{|j|}}. \tag{11}$$

We refer to the right-hand side of (11) as *critical ratio* and denote it by  $\Theta$  in the rest of the paper. The condition for the stability of the neural system then becomes

$$\gamma < \Theta. \tag{12}$$

Since  $\gamma w'_{|j|}$  is the  $j$ th inhibitory weight, an alternate way to express the stability condition (12) is

$$\frac{\text{Sum of lateral inhibitory weights}}{\text{Sum of excitatory weights}} < \frac{1}{2}.$$

Thus, if the sum of lateral inhibitory weights for a neuron is less twice the sum of its excitatory weights, the system is stable. Note that  $\Theta$ , as defined by (11), is a function of only the network connectivity specified by constants  $\tau$  and  $\rho$  and the weights determined by the relative distance between the source and the destination neurons. The constant nature of

$\Theta$  allows us to characterize network stability rather easily in the rest of the paper.

#### 4. Simulation results

We used MATLAB programs for all our simulations. In all simulation we used the same number of neurons,  $N = 40$ . In order to characterize the effect of input discontinuities on the output, we chose an input stimulus that has a single edge sufficiently far from the boundaries of the neural network. This edge was located between neurons 20 and 21, i.e.,  $x_i(t) = 55$ , for  $1 \leq i \leq 20$  and  $x_i(t) = 65$ , for  $21 \leq i \leq 40$ . We also assumed that there is only one layer of neurons. We used 500 iterations in each simulation run to allow the system to stabilize, if at all. We did two sets of simulations: with self-inhibition and without any self-inhibition; but report here only the results with self-inhibition. Systems without self-inhibition showed the same qualitative behavior. Particularly, when the number of connections to a neuron ( $n_i$  or  $n_e$ ) was large, both sets of simulations gave identical outputs. For small number of connections, networks with little or no self-inhibition produced much larger edge enhancement.

We used three weight distributions that we believe are probable in biological systems. In each case, the connectivity of the neural system and the weight ratio  $\gamma$  were varied and their effect on the critical ratio and output was determined. In order to parametrize the edge enhancement, we define the *edge enhancement* as the ratio of the difference in the stable maximum and minimum outputs

to the input edge amplitude. Simulations show that edge enhancement is independent of the value of inputs or the magnitude of edge.

Following subsections present the simulation results.

##### 4.1. Uniform weight distribution

In this set of simulations, all the excitatory weights ( $w_i$ ) were assumed to be equal and so were the inhibitory weights ( $\gamma w'_i$ ). Further, without loss of generality, these weights may be chosen to be 1, i.e.,

$$w_j = 1 \quad \text{for } -\rho \leq j \leq \rho,$$

$$w'_j = 1 \quad \text{for } -\tau \leq j \leq \tau.$$

Fig. 4 shows the input/output behavior of such a system with  $n_i = n_e = 3$ . From this figure one can see the criticality of the weight ratio in keeping the neural system stable. As soon as the weight ratio exceeds  $\Theta$ , the system oscillates with disproportionate magnitude. In Fig. 4(d), a weight ratio of mere 1% more than the critical ratio  $\Theta$  causes the output to oscillate about four orders of magnitude larger than the input discontinuity after 500 iterations.

The critical ratio dependence on the number connections is shown in Fig. 5. One can see that the critical ratio increases with increasing number of excitatory connections and decreasing number of inhibitory connections. But when the number of excitatory connections equals the number of inhibitory connections,  $\Theta$  approaches 0.5 as the number of connections becomes larger.

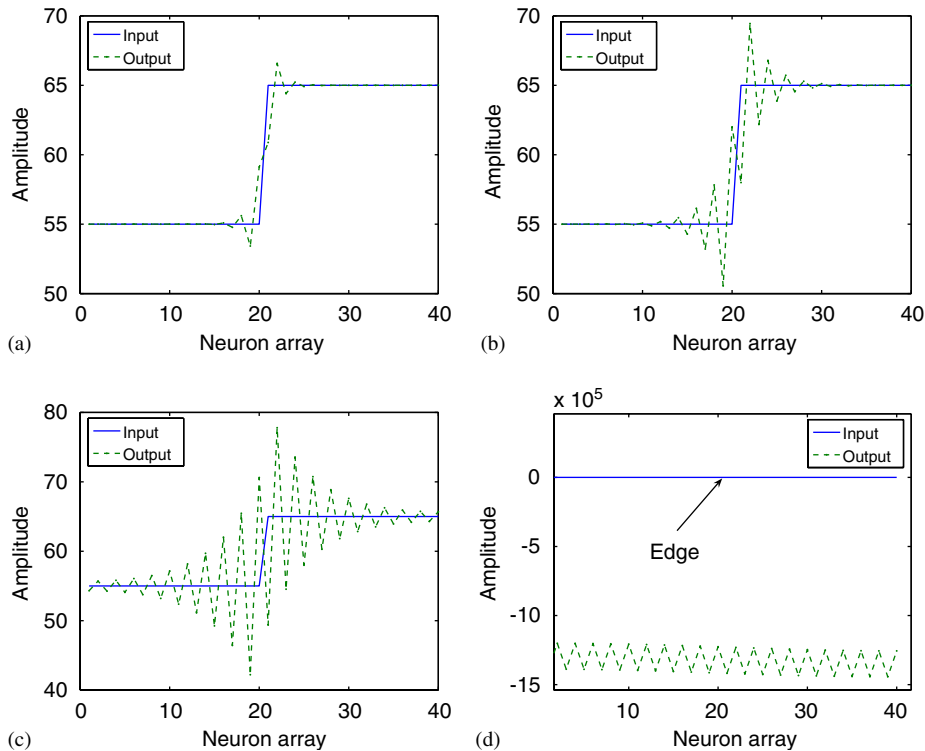


Fig. 4. Response of a neural system with uniform weights for  $n_i = n_e = 3$ . Notice how the system becomes unstable when  $\gamma$  exceeds  $\Theta = 0.75$ . The edge enhancement increases with increase in  $\gamma$ . (a)  $\gamma = 0.8\Theta$ , (b)  $\gamma = 0.95\Theta$ , (c)  $\gamma = 0.99\Theta$  and (d)  $\gamma = 1.01\Theta$ .

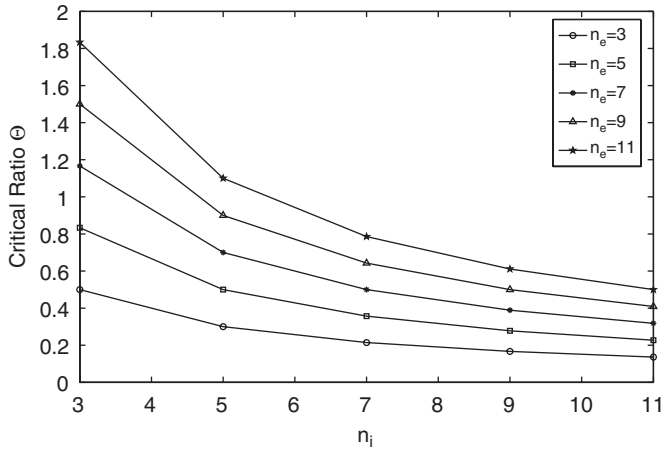


Fig. 5. Dependence of the critical ratio  $\Theta$  on number of inhibitory connections ( $n_i$ ) and excitatory connections ( $n_e$ ) for uniform weight distribution.

Fig. 4 also shows that as the weight ratio approaches the critical ratio, the edge enhancement increases, the rise being the sharpest just before the system becomes unstable. This dependence of edge enhancement on the weight ratio is shown in Fig. 6.

4.2. Inversely linear weight distribution

Our second set of simulations assumed signal loss along the length of synapses and axons. We therefore used weights that are inversely proportional to the length of the connection. Assuming unit distance between neighboring neurons and unit distance between neuron layers, we got

$$w_j = \frac{1}{|\sqrt{1+j^2}|} \quad \text{for } -\rho \leq j \leq \rho,$$

$$w'_j = \frac{1}{|j|} \quad \text{for } -\tau \leq j \leq \tau, j \neq 0 \text{ and } w'_0 = 1.5.$$

The behavior of this neural system with respect to stability was similar to the one described in Section 4.1 and shown in Fig. 4. The dependence of the critical ratio on  $n_e$  and  $n_i$  in this case is shown in Fig. 7. A neural system in this case has a much lower critical ratio than one with uniform weights with the same number of connections. Therefore, the signal losses within the neuron connections significantly reduce the range of weight ratio  $\gamma$  to keep the neural system stable.

The dependence of edge enhancement on  $\gamma$  for this weight distribution is shown in Fig. 8. One can see that for the same connectivity, the edge enhancement in this case is much smaller than in the case of uniform weights. Thus, loss of signal along the neural connections affects both the stability and the edge enhancement adversely.

4.3. Normal weight distribution

In the third set of simulations we assumed the weights to have a normal distribution. As before, we let the weights be

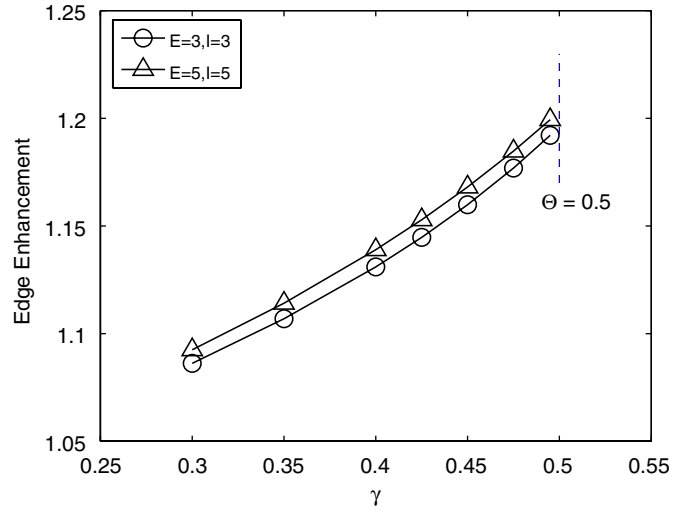


Fig. 6. Edge enhancement as a function of  $\gamma$  in case of uniform weight distribution for two network connectivities. Note that the edge enhancement increases with  $\gamma$  and is largest just before  $\gamma$  exceeds  $\Theta$ .

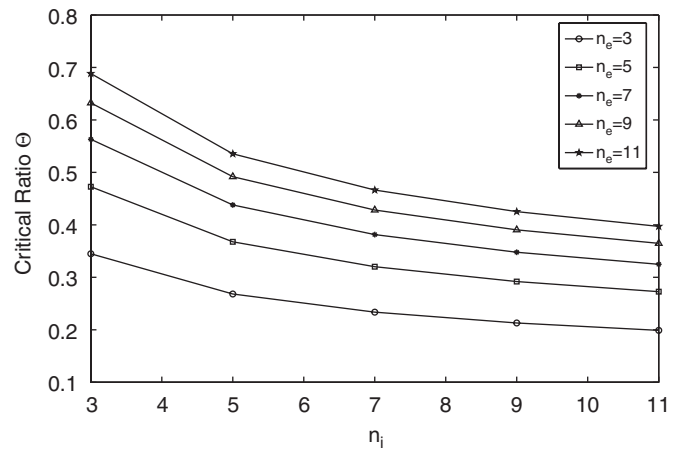


Fig. 7. Dependence of the critical ratio  $\Theta$  on number of inhibitory connections ( $n_i$ ) and excitatory connections ( $n_e$ ) for inversely linear weight distribution.

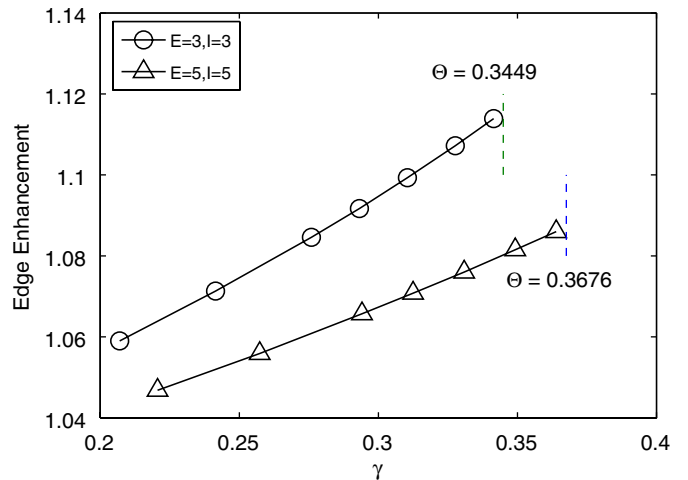


Fig. 8. Edge enhancement as a function of  $\gamma$  in case of inversely linear weight distribution for two network connectivities. Note the similarity with the curves in Fig. 6.

functions of the distance between the neurons. In addition, we choose large  $\rho$  and  $\tau$  so as to span all the neurons in a layer. However, with the standard deviations we chose, the distributions fall off sharply and there are no *edge effects* to consider. Thus, in this case, the weights become

$$w_j = \frac{1}{\sqrt{2\pi\sigma_e}} e^{-(1+j^2)/2\sigma_e^2} \quad \text{for } -\rho \leq j \leq \rho,$$

$$w'_j = \frac{1}{\sqrt{2\pi\sigma_i}} e^{-j^2/2\sigma_i^2} \quad \text{for } -\tau \leq j \leq \tau, j \neq 0 \text{ and } w'_0 = 0.5,$$

where  $\sigma_e$  and  $\sigma_i$  denote the standard deviations of the excitatory and inhibitory weight distributions, respectively. This allows us to use a connectivity strength that drops off gradually as we move further away from a neuron. This is in sharp contrast to the earlier two cases where the connectivity strength dropped abruptly beyond a chosen number of neurons. In this case, the weight distribution can be made flatter or narrower by increasing or decreasing the standard deviation. This allows us to control the sphere of influence of each neuron on its neighbors to a greater degree than the other two distributions. When  $\sigma_e \rightarrow \infty$  and  $\sigma_i \rightarrow \infty$ , the normal distribution degenerates into a uniform distribution.

The dependence of critical ratio on the standard deviations  $\sigma_e$  and  $\sigma_i$  in case of the normal weight distribution is shown in Fig. 9. This figure shows that increasing  $\sigma_i$  decreases the critical ratio. Thus, inhibitory influence from more neurons reduces the range of weight ratio over which the neural system is stable. On the other hand, increasing  $\sigma_e$  allows more excitatory connections to affect the output of a neuron and increase the critical ratio.

The edge enhancement in the case of the normal weight distribution is shown in Fig. 10. It is interesting to note that one gets substantial edge enhancement in the case of normal weight distribution. Further, this edge enhancement increases with smaller standard deviations of the weight profiles. This is in line with the earlier two weight distributions, in which a smaller number of connections tended to give a larger edge enhancement.

### 5. Other effects near the critical region

As has been discussed earlier, the relationship between  $\gamma$  and  $\Theta$  determines the stability of the neural network of Fig. 1 as well as the value of the edge enhancement. Our simulations show that the value of  $\gamma$  relative to that of  $\Theta$  plays a greater role in deciding many other properties of neural networks as well. Interestingly, as  $\gamma \rightarrow \Theta$ , the system behavior changes rapidly and other phenomena such as hysteresis become evident. An example of this rapid change can be seen from the perturbations around the input edge as  $\gamma$  approaches the critical ratio in Fig. 4. These radical changes are even more prominent in the absence of the self-inhibition. For example, in the case of inversely linear weight distribution, with no self-inhibition and

$n_e = n_i = 3$ , the edge enhancement is about 1.3 when  $\gamma = 0.9\Theta$  and 2.3 when  $\gamma = 0.99\Theta$ .

An edge in the input produces perturbations in the system response (see Fig. 4). We also observe that these perturbations spread laterally over a larger number of neurons as  $\gamma$  increases; the increase being more dramatic as  $\gamma$  nears the critical ratio. Table 1 shows this behavior.

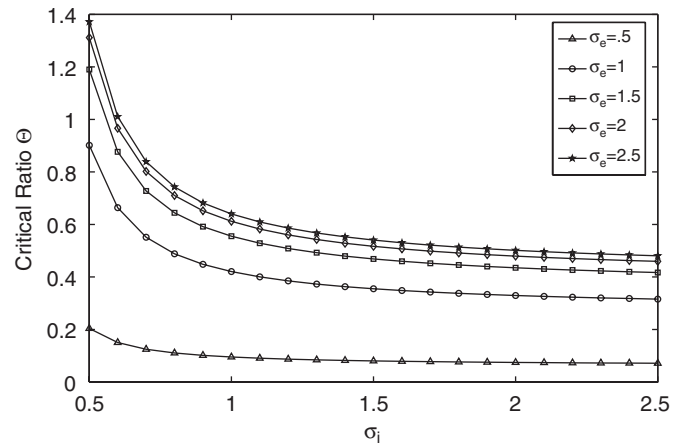


Fig. 9. Dependence of the critical ratio  $\Theta$  on the standard deviations of the inhibitory weights ( $\sigma_i$ ) and the excitatory weights ( $\sigma_e$ ) in case of the normal weight distribution.

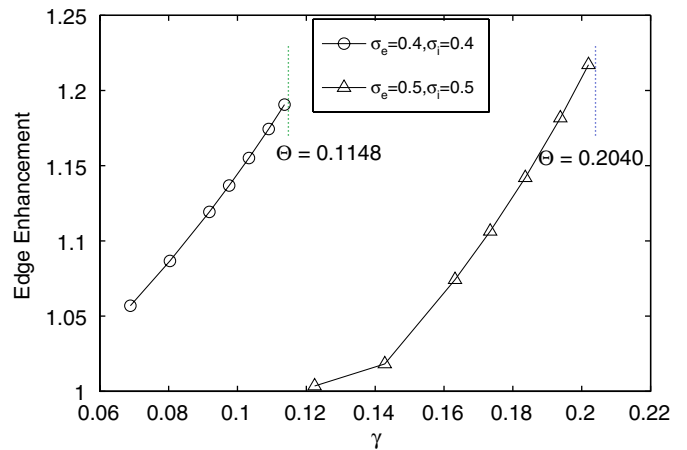


Fig. 10. Edge enhancement as a function of  $\gamma$  in case of a normal weight distribution for two network connectivities. Note the similarity with the curves in Figs. 6 and 8.

Table 1

Spread of perturbations in the system response because of an edge in the input pattern as  $\gamma$  approaches the critical ratio  $\Theta$

$\gamma$	Number of neurons affected by perturbations
$0.3\Theta$	5
$0.5\Theta$	5
$0.8\Theta$	7
$0.99\Theta$	11

The case illustrated here uses uniform weights,  $n_i = n_e = 5$ .

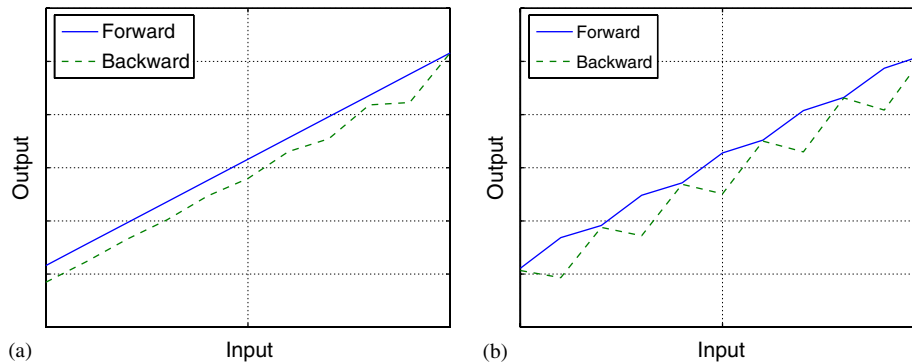


Fig. 11. The hysteresis in the neural system output when (a)  $\gamma = 0.8\Theta$  and (b)  $\gamma = 0.99\Theta$ . The case illustrated uses uniform weights with  $n_i = n_e = 5$ . The same input is applied to all the neurons. Solid line indicates the neural network output as the input is increased, the dotted line shows the output as the input is decreased.

Jacobs and Werblin [11] have observed experimentally that a high-illumination narrow spike stimulus produced ridges in the retinal output which spread laterally. This phenomenon can be explained in the context of our model as follows. It is known that stimulus intensity alters the balance between excitation and inhibition in visual cortex, and in particular, it suppresses the excitatory response while enhancing the inhibitory response [20]. In other words, a high-illumination spike such as the one used by Jacobs and Werblin may indeed cause  $\gamma$  to increase, and even bring it close to the critical ratio  $\Theta$ , thus producing a lateral spread of the output spike. As the ridge progresses, it changes the  $\gamma$  of the surrounding neurons, which in turn spread the ridge further.

The  $\gamma$ -dependent feedback in the neural system (see Fig. 3) produces hysteresis effects, particularly when  $\gamma$  is close to the critical ratio. Fig. 11 shows a typical behavior of the system for two values of  $\gamma$ . During these simulations, all the neurons were applied the same input. The input was either linearly increased or decreased with time and the output of the neural system was recorded. Note the substantial difference in the output for the same value of input depending upon whether the input was increasing or decreasing. Note that for low values of  $\gamma$ , hysteresis effects are not observed.

Cai et al. have demonstrated hysteresis by using kinetic theory to a mixture of simple (linear) and complex (non-linear) neurons [4]. Our relatively simple model also displays hysteresis albeit only when  $\gamma$  is very close to  $\Theta$ .

## 6. Conclusions

This paper deals with the imbalance between the strengths of the inhibitory and excitatory phenomena in the neuron. We assume that the effect of neighboring neurons on any neuron is dependent upon their distances from the neuron, but given the same distance, an inhibitory influence is  $\gamma$  times stronger than an excitatory influence. In terms of neural networks this implies that the weights of inhibitory connections are  $\gamma$  times larger than the excitatory connections. We have assumed only lateral inhibition. We have considered three very different weight

functions and the overall conclusions of this work seem to be independent of them.

From the mathematical analysis and the simulations we observe that in stable neural networks,  $\gamma$  has upper bound which we call the *critical ratio*  $\Theta$ . This bound  $\Theta$  is dependent only on the network connectivity and the weight functions. When  $\gamma < \Theta$ , the neural system is able to enhance any discontinuities in the input stimulus. If  $\gamma$  exceeds  $\Theta$  even minimally, the system output instantly becomes erratic. The edge enhancement increases rapidly as the system approaches instability (i.e., as  $\gamma \rightarrow \Theta$ ). The number of neurons affected by the input discontinuity also grows at the same time. The spacial discontinuity in the stimulus produces stable periodic patterns around the discontinuity region. Such periodic patterns have been observed by others in intracortical neuronal fields [10]. Simulations show that edge enhancement is independent of the actual values of the inputs.

The stability region ( $\gamma < \Theta$ ) depends on the localization of connections. If there are very few lateral inhibitory connections or a large number of excitatory connections from a lower layer, then the stability region is wider. In other words, in this case, a larger amount of imbalance between the excitatory and inhibitory strengths may be tolerated. For  $\gamma$  values close to  $\Theta$  (but less than  $\Theta$ ), the system exhibits hysteresis. Many of the system properties change at a rapid rate when  $\gamma \rightarrow \Theta$  creating unwanted anomalies. Determination of the stability region and the critical ratio  $\Theta$  identified here will help avoid such situations and achieve a balance between the excitatory and inhibitory strengths for well-behaved neural networks.

## Acknowledgment

The authors wish to thank the reviewers for suggesting several improvements to the manuscript.

## References

- [1] D.J. Amit, N. Brunel, Model of global spontaneous activity and local structured activity during delay periods in the cerebral cortex, *Cereb. Cortex* 7 (1997) 237–252.

- [2] E.A. Benardete, E. Kaplan, The receptive field of the primate p retinal ganglion cell, i: linear dynamics., *Visual Neurosci.* 14 (1) (1997) 169–185.
- [3] A.N. Burkitt, Balanced neurons: analysis of leaky integrate-and-fire neurons with reversal potentials, *Biol. Cybern.* 85 (4) (2001) 247–255.
- [4] D. Cai, L. Tao, M. Shelley, D.W. McLaughlin, An effective kinetic representation of fluctuation-driven neuronal networks with application to simple and complex cells in visual cortex, *Proc. Natl. Acad. Sci.* 101 (20) (2004) 7757–7762.
- [5] M. Carandini, D.J. Heeger, J.A. Movshon, Linearity and normalization in simple cells of the macaque primary visual cortex, *J. Neurosci.* 17 (21) (1997) 8621–8644.
- [6] C. Enroth-Cugell, J.G. Robson, D.E. Schweitzer-Tong, A.B. Watson, Spatio-temporal interactions in cat retinal ganglion cells showing linear spatial summation, *J. Physiol.* 347 (1983) 297–307.
- [7] R. Galambos, H. Davis, Inhibition of activity in single auditory nerve fibers by acoustic simulations, *J. Neurophysiol.* 7 (1944) 287–304.
- [8] B.S. Gutkin, C.E. Smith, Conditions for noise reduction and stable encoding of spatial structure by cortical neural networks, *Biol. Cybern.* 82 (6) (2000) 469–475.
- [9] H. Hartline, F. Ratliff, *Studies on Excitation and Inhibition in the Retina*, The Rockefeller University Press, New York, 1974.
- [10] A. Hutt, M. Bestehorn, T. Wennekers, Pattern formation in intracortical neuronal fields, *Network: Comput. Neural Syst.* 14 (2003) 351–368.
- [11] A.L. Jacobs, F.S. Werblin, Spatiotemporal patterns at the retinal output, *J. Neurophysiol.* 80 (1) (1998) 447–451.
- [12] D.G. Kelly, Stability in contractive nonlinear neural networks, *IEEE Trans. Biomed. Eng.* 37 (3) (1990).
- [13] B.B. Lee, J. Pokorny, V.C. Smith, J. Kremers, Responses to pulses and sinusoids in macaque ganglion cells, *Vision Res.* 34 (23) (1994) 3081–3096.
- [14] L. Maffei, A. Fiorentini, The visual cortex as a spatial frequency analyzer, *Vision Res.* 13 (7) (1973) 1255–1267.
- [15] V.B. Mountcastle, The columnar organization of the neocortex, *Brain* 120 (1997) 701–722.
- [16] M.N. Shadlen, W.T. Newsome, Noise, neural codes and cortical organization, *Curr. Opin. Neurobiol.* 4 (4) (1994) 569–579.
- [17] M.N. Shadlen, W.T. Newsome, The variable discharge of cortical neurons: implications for connectivity, *J. Neurosci.* 18 (10) (1998) 3870–3896.
- [18] R.S. Verga, *Gerschgorin and His Circles*, Springer, Berlin, 2004.
- [19] M. Wehr, A.M. Zador, Balanced inhibition underlies tuning and sharpens spike timing in auditory cortex, *Lett. Nat.* 426 (2003) 442–446.
- [20] M. Welky, K. Kandler, D. Fitzpatrick, L.C. Katz, Patterns of excitation and inhibition evoked by horizontal connections in visual cortex share a common relationship to orientation columns, *Neuron* 15 (3) (1995) 541–552.



**Pradeep Arkachar** received his B.E. in Electronics and Communications from Mysore University in 2000. He received his M.S. in Electrical Engineering from Lehigh University in 2003. His interests are in the fields of signal processing, bioengineering and economics. He is currently working at Ease Diagnostics as embedded electronics design engineer.



**Meghanad D. Wagh** got his B.Tech and Ph.D., both in Electrical Engineering, from Indian Institute of Technology, Bombay. His research interests include algorithms and architectures for high-speed applications and alternate computing paradigms. He is currently an associate professor of Computer and Electrical Engineering at Lehigh University.